EBioMedicine 46 (2019) 160–169

Contents lists available at ScienceDirect

EBioMedicine

journal homepage: www.ebiomedicine.com

EBioMedicine
Published by THE LANCET

Research paper

Radiomic analysis for pretreatment prediction of response to neoadjuvant chemotherapy in locally advanced cervical cancer: A multicentre study

Caixia Sun [a,b,1], Xin Tian [c,1], Zhenyu Liu [b,d,1], Weili Li [c,1], Pengfei Li [c], Jiaming Chen [c], Weifeng Zhang [c], Ziyu Fang [c], Peiyan Du [c], Hui Duan [c], Ping Liu [c,**], Lihui Wang [a,***], Chunlin Chen [c,**], Jie Tian [b,d,e,f,*]

[a] Key Laboratory of Intelligent Medical Image Analysis and Precise Diagnosis of Guizhou Province, School of Computer Science and Technology, Guizhou University, Guiyang, China
[b] CAS Key Laboratory of Molecular Imaging, Institute of Automation, Chinese Academy of Sciences, Beijing, China
[c] Department of Gynaecology and Obstetrics, Nanfang Hospital, Southern Medical University, Guangzhou, China
[d] School of Artificial Intelligence, University of Chinese Academy of Sciences, Beijing, China
[e] Beijing Advanced Innovation Center for Big Data-Based Precision Medicine, School of Medicine, Beihang University, Beijing, China
[f] Engineering Research Center of Molecular and NeSuro Imaging of Ministry of Education, School of Life Science and Technology, Xidian University, Xi'an, Shaanxi, China

ARTICLE INFO

Article history:
Received 4 June 2019
Received in revised form 5 July 2019
Accepted 18 July 2019
Available online 6 August 2019

Keywords:
Radiomics
Magnetic resonance imaging
Neoadjuvant chemotherapy
Locally advanced cervical cancer

ABSTRACT

Background: We aimed to investigate whether pre-therapeutic radiomic features based on magnetic resonance imaging (MRI) can predict the clinical response to neoadjuvant chemotherapy (NACT) in patients with locally advanced cervical cancer (LACC).

Methods: A total of 275 patients with LACC receiving NACT were enrolled in this study from eight hospitals, and allocated to training and testing sets (2:1 ratio). Three radiomic feature sets were extracted from the intratumoural region of T1-weighted images, intratumoural region of T2-weighted images, and peritumoural region of T2-weighted images before NACT for each patient. With a feature selection strategy, three single sequence radiomic models were constructed, and three additional combined models were constructed by combining the features of different regions or sequences. The performance of all models was assessed using receiver operating characteristic curve.

Findings: The combined model of the intratumoural zone of T1-weighted images, intratumoural zone of T2-weighted images,and peritumoural zone of T2-weighted images achieved an AUC of 0.998 in training set and 0.999 in testing set, which was significantly better ($p < .05$) than the other radiomic models. Moreover, no significant variation in performance was found if different training sets were used.

Interpretation: This study demonstrated that MRI-based radiomic features hold potential in the pretreatment prediction of response to NACT in LACC, which could be used to identify rightful patients for receiving NACT avoiding unnecessary treatment.

1. Introduction

Cervical cancer is one of the most frequent malignant tumours in women [1]. Standard therapeutic strategies for locally advanced cervical cancer (LACC) include radical hysterectomy (RH) or concurrent chemoradiation [2]. Preoperative neoadjuvant chemotherapy (NACT) is being increasingly investigated as alternative treatment strategy for locally advanced disease due to its ability to reduce the tumour volume and render unresectable tumours operable [3–5]. Chemotherapeutic responders could exhibit clinical survival benefit over patients undergone primary surgery [6,7]. Conversely, chemotherapeutic non-responders experience unnecessary chemotherapy-related toxicities and disease

* Correspondence to: J. Tian, CAS Key Laboratory of Molecular Imaging, Institute of Automation, Chinese Academy of Sciences, Beijing 100190, China.
** Corresponding author at: Department of Gynaecology and Obstetrics, Nanfang Hospital, Southern Medical University, 1838 Guangzhou Avenue North, Guangzhou, 510515, China.
*** Corresponding author at: Key Laboratory of Intelligent Medical Image Analysis and Precise Diagnosis of Guizhou Province, School of Computer Science and Technology, Guizhou University, No.2708 South Section of Huaxi Avenue, Guiyang, 550025, China.
E-mail addresses: lpivy@126.com (P. Liu), wlh1984@gmail.com (L. Wang), ccl1@smu.edu.cn (C. Chen), jie.tian@ia.ac.cn (J. Tian).
[1] These authors contributed equally to this work, and should be considered as co-first authors.

https://doi.org/10.1016/j.ebiom.2019.07.049

Research in context

Evidence before this study

We searched publications with the following terms on PubMed and Web of Science: "(radiomics OR texture analysis) AND (predict OR prediction) AND (response OR non-response) AND neoadjuvant chemotherapy AND locally advanced cervical cancer". The articles were not limited to English language publications and didn't have date restriction. There was no study research the prediction of response to neoadjuvant chemotherapy in locally advanced cervical cancer by radiomic analysis.

Added value of this study

Neoadjuvant chemotherapy (NACT) is being considered as an alternative treatment strategy for patients with locally advanced cervical cancer (LACC) due to its ability to reduce the tumour volume and render unresectable tumour operable. The chemotherapeutic responders could exhibit clinical survival benefit but non-responders undergone unnecessary treatment and worse prognosis. Therefore, accurate prediction of response to NACT in LACC is urgently need in order to implement personalized treatment for individual patient. Radiomic analysis based on magnetic resonance imaging has been used to predict the pathological complete response (pCR) to NACT in various types of cancers. However, no previous studies have devoted to predict the response to NACT in LACC based on radiomic analysis. We aim to investigate whether pre-therapeutic radiomic features can predict the clinical response to NACT in patients with LACC, which may be a potential tool to construct a treatment guide for individual patient.

Implications of all the available evidence

Our findings suggested that the radiomic is sufficient to serve as an effective tool to stratify LACC patients to allow for more appropriate initial treatment, showing promise in improving the management of LACC.

progression due to delays in effective treatment, which worsen the prognosis [8,9]. Accordingly, to optimize the treatment efficacy, only chemotherapeutic responders can be selected for implementing NACT-RH while non-responders should directly undergo concurrent chemoradiation. This scenario highlights the need for accurate identification of chemotherapeutic non-responders and responders prior to the initiation of therapy. An effective and clinically validated approach that pre-therapeutically predicts chemotherapeutic responsiveness is thereby crucial to individualize treatment strategies and facilitate appropriate patient stratification.

Magnetic resonance imaging (MRI) is recognized as the gold standard for monitoring the cervical tumour response to chemotherapy and allows determination of eligibility for subsequent resection [10–13]. Extensive evidence has indicated the value of MRI in evaluating or predicting early cervical cancer therapy response. Yin et al. [14] comfirmed that combining pre- and post-treatment MRI with the squamous cell carcinoma (SCC) antigen level was a reliable and sensitive measure for assessing the response to chemotherapy in patients with cervical cancer with high accuracy. In terms of cost-effectiveness and clinical practicality, MRI-based biomarkers are generally superior to some proposed clinicopathologic, genomic, or proteomic predictors of the NACT response. In addition, comparing quantitative parameters extracted from pre- and post-treatment functional MRI has been demonstrated to improve response assessment by detecting invisible biological properties of cervical tumour [15–17]. However, most research methods are conducted on a post-treatment basis and yield variable diagnostic performances, thereby restricting the utility in the initial decision making regarding NACT. Thus, novel means that allow for quantitative exploration of pretreatment MRI in order to differentiate non-responders and responders are urgently needed.

Radiomics, as a newly-proposed method, aims to evaluate tumour heterogeneity by extracting high throughput features from medical images that reflect the underlying pathophysiology [18–20]. These radiomic features capture distinct phenotypic differences and may have prognostic and predictive value across different diseases [21–24]. Emerging studies have demonstrated the excellent performance of radiomic models for predicting the pathological complete response (pCR) to NACT in rectal cancer [25,26]. Prediction of the pCR to NACT in breast cancer was successfully performed by radiomic analysis using pretreatment breast MRI in several studies [27,28]. In the field of cervical cancer, El Naqa et al. [29] reported the good predictive power of radiomic features in predicting individual chemoradiotherapy outcomes based on single centre small patient cohorts. However, most of the established predictive models were trained with a single centre dataset may have limited generalization capabilities. Until recently, Lucia et al. [30,31] further verified the prognostic role of pretreatment MRI-based radiomics in patients with LACC treated with definitive chemoradiation using external multicentre patient datasets. These studies provided the likelihood of employing radiomics in patients with cervical tumour for prediction of the response to NACT.

Based on the successful application of radiomics in other research areas, we hypothesized that pretreatment radiomic features would be effective in the prediction of the response to NACT in patient with LACC. Thus, in the present study, we aimed to construct a model for predicting the response to NACT by exploring multi-centric pretreatment MRI-based radiomic analysis, and validate the model with a multicentre dataset.

2. Materials and methods

2.1. Patients

This study design was approved by an institutional review board and waived the informed consent requirement. The patients of this retrospective multicentre study were enrolled in from eight centres between January 2009 and June 2018. In this study, 275 consecutive patients with histologically confirmed LACC who underwent NACT and had pretreatment MRI data were included. The recruitment of patients is described in the supplemental material and Fig. S1. In this study, patients were divided into training and testing sets according to the hospital they were recruited from. The training set consisted of 183 patients from five hospitals, including the first affiliated hospital of zhengzhou university, second affiliated hospital of zhengzhou university, nanfang hospital, yuncheng central hospital, affiliated hospital of qingdao university. The independent-testing set includes 92 patients from the remaining three hospitals, including the henan provincial people's hospital, army military medical university xinqiao hospital, yantai sulphur top hospital.

All of the included patients received cisplatin-based (70–75 mg/m2) chemotherapy intra-arterially or intravenously. The tumour volume was evaluated by a gynecological examination and pelvic MRI scan before each chemotherapy cycle and three weeks after NACT. Besides, the extent of change in tumour volume needs to be confirmed by pathological examination. When the patient's tumour shrinks to meet the surgical conditions, the patient would underwent Type III RH after one cycle of chemotherapy. The surgery was performed within 21 days after the end of the final cycle. In contrast, the patients who did not meet the surgical requirements received 1–2 cycles of chemotherapy every 21 days. In addition, radiotherapy was performed for patients with progressive diseases or those who experienced adverse side effects due to the toxicity of anti-tumour agents during or after NACT. In this study, patients from different centres underwent distinct courses of

NACT. Among these patients, 131 patients underwent one cycle of NACT, 126 patients underwent two cycles, and 18 patients had three cycles.

The short-term response was assessed by change in tumour volume according to the Response Evaluation Criteria in Solid Tumours (RECIST v.1.1) [32]. We defined responsivebess according to the various treatment courses of patients in this study as follows: patients with a complete response or partial response within two cycles of chemotherapy were considered as "responders" (chemo-sensitive), while those still with progressive disease or stable disease after two cycles of treatment were considered as "non-responders" (chemo-insensitive) regardless of the response after the final chemotherapy cycles. Thus, there were 204 responders and 71 non-responders among the 275 eligible patients.

2.2. Image acquisition and tumour masking

Pretreatment MRI examinations were performed within one week before the first cycle of NACT. The MRIs of training set combined five hospitals were performed with 3.0-T (Skyra, SIEMENS, Germany), 1.5-T (Signa Excite, GE, USA), 1.5-T (Optima MR 360, GE, USA), 1.5-T (Symphony Tim, SIEMENS, Germany) and 1.5-T (Signa HDxt, GE, USA). The MRIs of testing set combined three hospitals were performed with 3.0-T (TrioTim, SIEMENS, Germany), 3.0-T (Signa HDxt, GE, USA) and 3.0-T (Signa Excite, GE, USA). The MRI protocols of each hospitals included axial TSE T2-weighted fat-suppressed sequence and T1-weighted sequence but have some different. The comprehensive parameters of MR image acquisition of each hospital are provided in Table S1.

The pretreatment MRI sequences were collated for tumour segmentation and feature generation. The regions of interest (ROIs) of images were manually delineated on each slice (using ITK-SNAP software: www.itksnap.org) containing the tumour mass on T1-weighted imaging (T1WI) and fat suppression on T2-weighted imaging (T2WI). The T2WI series delineated the peritumoural area in addition to the intratumoural region. The inter- and intra-observer reproducibility for ROI-based feature extraction were analysed in a blind fashion by two radiologists with 7 (reader 1) and 10 (reader 2) years of experience. More details regarding reproducibility are presented in the supplementary material.

2.3. Radiomic feature extraction and selection

Radiomic feature extraction was conducted using the in-house toolbox developed by MATLAB 2016b (Mathworks, Natick, MA, USA). Before the feature extraction, each slice of MR images was normalized with z-score so that get a standard normal distribution of image intensities. Then, Six hundred and forty seven predefined features were extracted from each ROI of the MR images: 17 first order statistic features, eight shape features, 54 textural features, and 568 wavelet features (Table S2). The 647 features were extracted from the intratumoural region on T1WI, intratumoural region on T2WI, and peritumoural region on T2WI. Finally, a total of 1941 radiomic features were extracted from each patient. The extracted features are reproducible and match the benchmarks of IBSI [33,34]. Each feature of each patient in training or testing sets was normalized with z-score in order to remove the effect of different MRI scanners [35].

Introducing a large number of features to the prediction model may cause over-fitting, thereby reducing the performance of the model on another dataset. To reduce the dimensionality of features, we adopted recursive feature elimination based on a support vector machine (SVM-RFE) to select top features in three feature sets [36]. Previous studies [37,38] have demonstrated that SVM-RFE was excellent on radiomic analysis for feature selection, which aims to select the features that best fit the current classification task. The SVM-RFE is used to determine the optimal subset of features through calculating the classified accuracy with different combinations of features by SVM.

2.4. Single sequence model construction and validation

To constructed the radiomic models, the previously selected features were used as inputs to random forest (RF) models. These models were constructed based on the training set, and a grid search with three-fold cross-validation was applied to set the hyperparameters of the RF models. After the models were constructed, their ROC curves [39] were plotted to assess and compare the quantitative performance of different models.

Three single MRI sequence models were constructed (T1WI with the intratumoural zone, T2WI with the intratumoural zone, T2WI with the peritumoural zone) within the training set, and the performance of the models was validated with testing set.

2.5. Combined model construction and validation

Three different combined radiomic models were generated by combining the features of different sequences or tumour regions, including combination of intratumoural T1WI and intratumoural T2WI, T2WI sequence with both intratumoural and peritumoural regions, and T1WI and T2WI sequences with all regions (multi-sequence). It should be emphasized that the construction process of the combined models was same as that for single sequence models. The pipeline of the entire experiment is presented in Fig. 1.

In addition, to assess the robustness of the models, three additional different training sets were composed of patients from three random combinations of hospitals, and the patients from remaining hospitals were assigned to testing sets. The hospital combination between each group of training and testing sets were different, the combinations also differ from original training and testing sets, which to verify whether the predictive power of the model depends on the patient composition of the training set. As indicated in Table S3, all training and testing sets comprised a similar number of patients. The training and testing process of the three patient groups were used the same features selection and model construction strategy as in the previous experiment. Then the robustness of models for NACT response prediction was evaluated by the ROC curve.

2.6. Clinical factor and radiomic model

A clinical model was constructed based on the subset of patients whose clinical information (age, FIGO stage, and gross type) is available. The process of clinical model construction was consistent with radiomic model. Then, as a comparison, evaluating the predictive result of the patients in radiomic model.

2.7. Statistical analysis

Descriptive statistics of continuous variables are presented as the mean ± standard deviation, and the Student's *t*-test was applied to compare the difference between groups. The p value of the χ^2 test was used to illustrate differences between qualitative variables. Generally, p values were two sided, and $p < .05$ was considered statistically significant. Comparison of qualitative variables between groups was conducted with a one-way analysis of variance. The cut-off values of models were determined according to the Youden index [40] of training sets to quantize the discrimination ability of models. Quantitative comparison of AUCs was made with the Delong test [41]. The predictive accuracy of models was evaluated by balanced accuracy [42] due to the imbalanced ratio between responders and non-responders. All experiments and statistical analyses were implemented with python 2.7.

2.8. Data statement

The experimental data are not available for public access due to patient privacy concerns but can be obtained from the corresponding

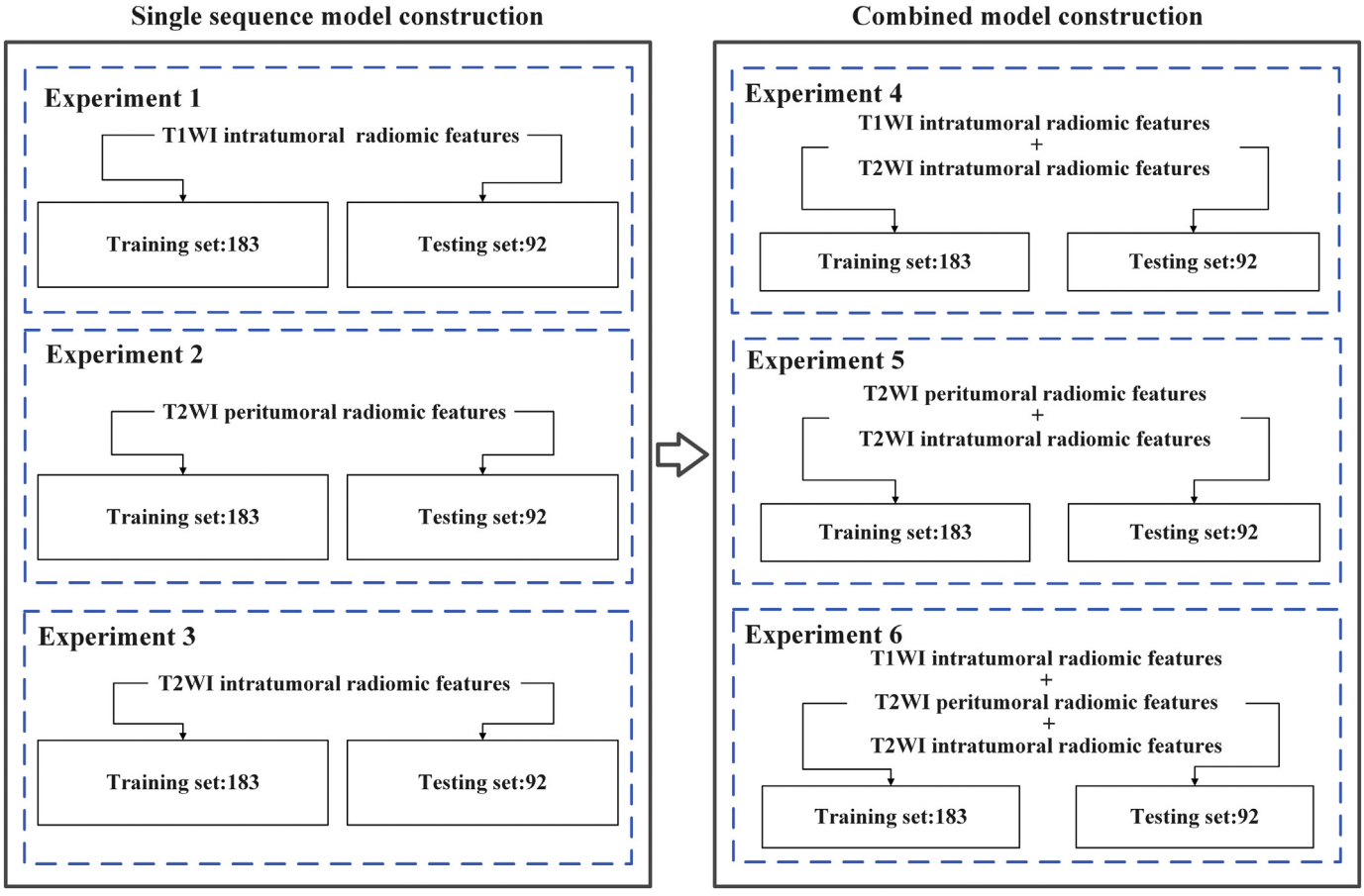

Fig. 1. Study design. Left block diagram is procedure of single sequence radiomic model construction. Right block diagram is procedure of combined model construction. T1WI, T1-weight imaging; T2WI, T2-weighted imaging.

author on reasonable request approved by the institutional review board of Nanfang Hospital.

3. Results

3.1. Clinical characteristics

The clinical characteristics of patients are provided in Table 1. In these two sets, no significant difference ($p > .05$) was observed in age between responders and non-responders. Meanwhile, the NACT response was found to be significantly correlated with FIGO stage in the training set but not in the testing set. In addition, the clinical characteristic of patients for assessing the model's stability are illustrated in Table S4 and Table S5. The clinical characteristic of patients for coustructing clinical model are listed in Table S6.

3.2. Feature selection

After feature selection in the training set, ten, two and four image features were finally selected from the T1WI, and the intratumoural and peritumoural zones of T2WI images, respectively. The information of selected features is listed in Table S7. From these features, three representative feature maps for responders and non-responders to NACT are illustrated in Fig. 2, namely the feature of low grey-level zone emphasis of the grey-level size zone matrix on T1WI, neighborhood grey-tone difference matrix (NGTDM)_busyness feature in the intratumoural

Table 1
Clinical characteristics of patients in the training and testing sets.

Characteristics	Training set			Testing set		
	Responders	Non-responders	*p*	Responders	Non-responders	*p*
Age (years, mean ± SD)	47.9 ± 8.1	46.1 ± 9.2	0.227	50.9 ± 7.7	50.7 ± 9.2	0.918
FIGO stage			<0.001*			0.349
IB2	57 (38.3%)	11 (32.4%)		7 (12.7%)	3 (8.1%)	
IIA-IIA2	62 (41.6%)	6 (17.6%)		16 (29.1%)	7 (18.9%)	
IIB-IIIB	30 (20.1%)	17 (50.0%)		32 (58.2%)	27 (73.0%)	

Note: The chi-square test was used to compare the difference in categorical variables (FIGO stage), while a Student's *t*-test was used to compare the difference in age.
* $P < .05$. SD, standard deviation.

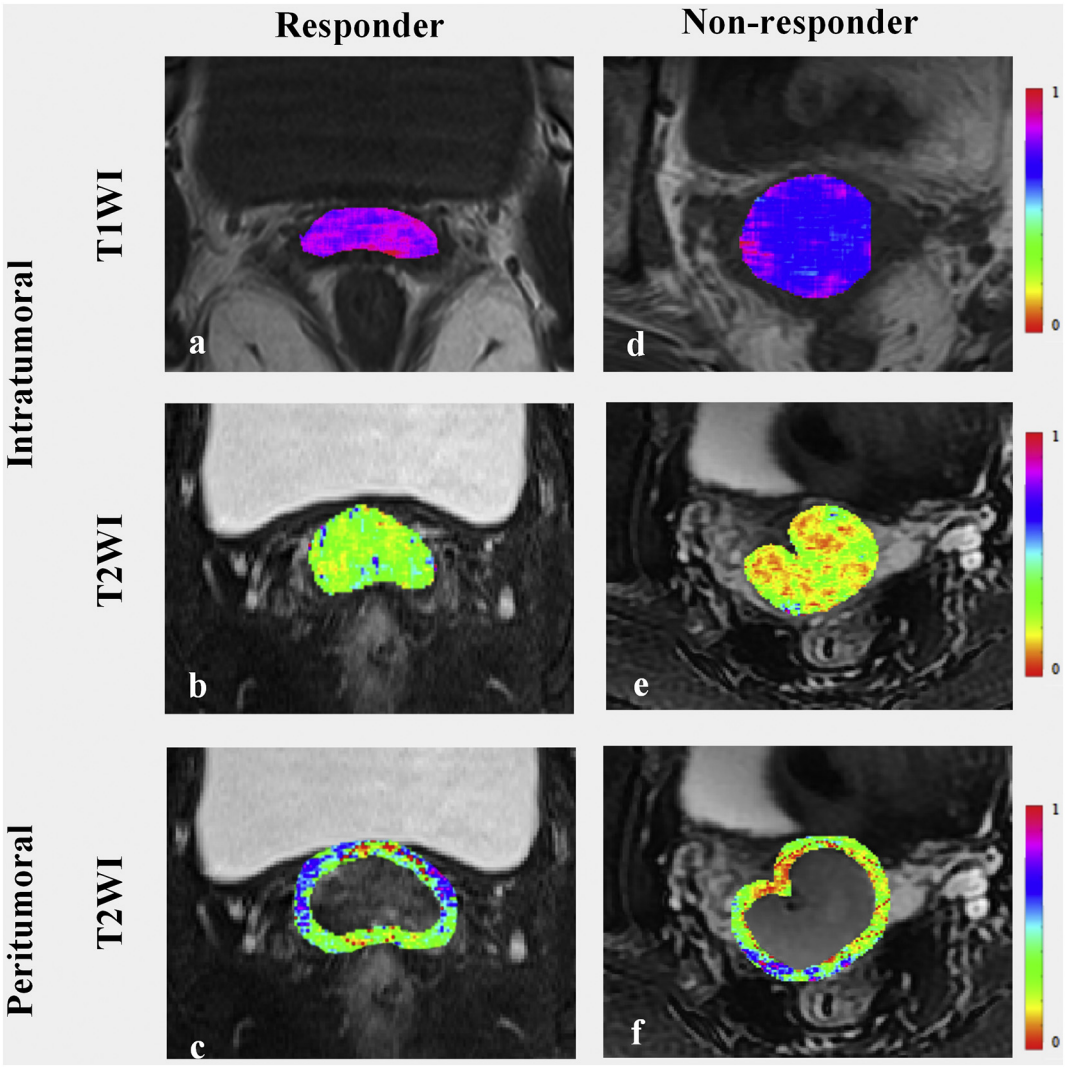

Fig. 2. Feature expression maps for top radiomic features. (a) and (d) are Coif3_glszm_ low grey-level zone emphasis features of intratumoural T1WI of patients. (b) and (e) are Coif1_ngtdm_busyness features of features of intratumoural T2WI of patients. (c) and (f) are Coif3_ngtdm_complexity features of peritumoural T2WI of patients. T1WI, T1-weight imaging; T2WI, T2-weighted imaging.

zone of T2WI, and NGTDM_complexity feature in the peritumoural zone of T2WI. It can be observed that all features of the responders have higher expression than those of non-responders.

3.3. Single sequence model construction and validation

Based on the selected features, the radiomic models for each sequence with different tumour regions were constructed using the RF method, including the T1WI sequence with the intratumoural region, a T2WI sequence with the intratumoural region, and a T2WI sequence with the peritumoural region.

The ROC curves of the above-mentioned models in the training and testing sets are presented in Fig. 3a–b. Using the radiomic features extracted from the intratumoural region, the AUCs for single-sequence (T1WI or T2WI) models were > 0.96 in the training set and > 0.94 in the testing set. However, using the radiomic features extracted from the peritumoural region, the AUC for the single sequence (T2WI) model could reach 0.975 in the training set and 0.98 in the testing set. The specificity of three models was show good performance in training and testing sets. Different from specificity, the sensitivity of these models was >84% in the training set but <77% in the testing set. To further evaluate the performance of different models, the quantitative metrics are provided in Table 2.

3.4. Combined model construction and validation

The three combined models were then constructed by combining features of different sequences or regions, including intumoural combination of T1WI and T2WI, T2WI with both peritumoural and intratumoural regions, and T1WI and T2WI with all tumour regions (multi-sequence). The performance of the three combined models are illustrated in Fig. 3c–d. From Table 3, we observed that, using the combination of radiomic features extracted from intratumoural T1WI and intratumoural T2WI, the AUC for the combined model was 0.967 and 0.980 in the training and testing sets, respectively. Meanwhile, another model, combining both tumour regions of T2WI, yielded an AUC of 0.991 in the training set and 0.994 in the testing set. Considering the significance of multi-sequence images in feature expression and compensation, the response prediction using all radiomic features extracted from multi-sequences images was evaluated, the AUC of which was further increased to 0.998 in the training set and 0.999 in the testing set. Specifically, the combined model of intratumoural regions (T1WI and T2WI) and combined model of both regions (T2WI) yielded good sensitivity in the training set but exhibited an unsatisfactory performance in the testing set. However, the multi-sequence model not only exhibited excellent sensitivity and specificity in the training set, but also performed satisfactorily in the testing set.

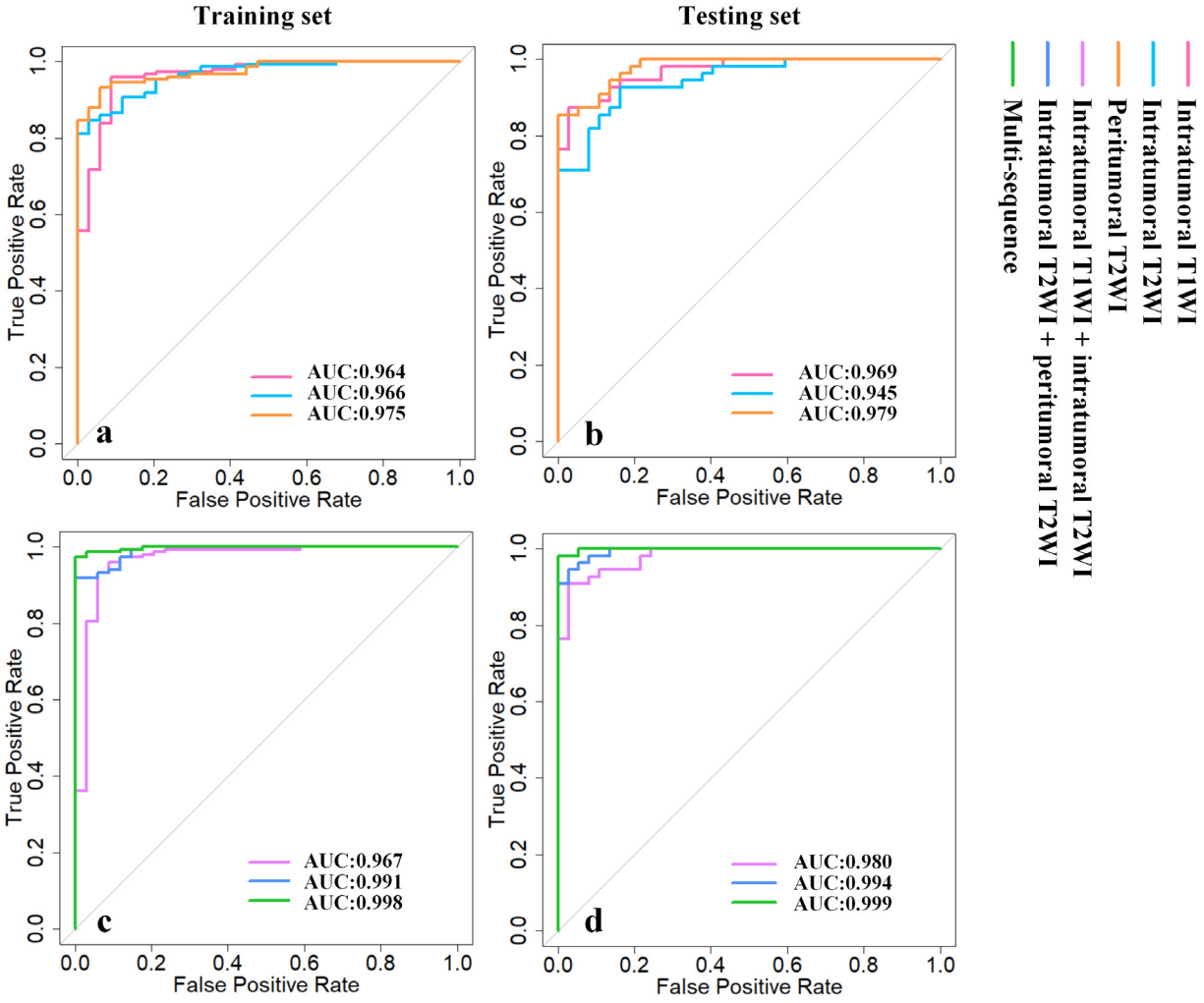

Fig. 3. Comparison of ROC curves of different models. (a) and (b) are ROC curves of single sequence models in training and testing sets. (c) and (d) are ROC curves of combined models in training and testing sets. ROC receiver operating characteristic; AUC area under receiver operating characteristic curve; T1WI, T1-weight imaging; T2WI, T2-weighted imaging.

3.5. Model comparison

The performance of the multi-sequence model was significantly increased ($p < .05$) compared to most single sequence models in both sets (Fig. 4). In the comparison of combined models in the training set, the AUC of the multi-sequence model was higher ($p < .05$) than that of the other combined models. Further, in the testing set, there were no significant differences in the AUCs among the three combined models.

Furthermore, for each group of training and testing sets consisting of parients from different combination of hospitals, the three ROC curves (Fig. 5) of the combined models were robust. The performances of the models in the three combination groups have no significantly difference (Table S8). Similar to the previous experimental results, the sensitivity and specificity of the multi-sequence model were more stable than those of the other combined models in both sets. This indicated that regardless of the source of the training data, the multi-sequence model exhibited robust and persistent performance.

3.6. Clinical factor and radiomic model

The clinical factors were identified as independent predictors for the response to NACT, including age, FIGO stage, gross type. Finally, only 169 and 63 patients have complete clinical information in training and testing sets. As shown in Fig. 6, the clinical model yielded AUCs of

Table 2
Performance of single sequence models.

Cohort	Model	ACC (%)	AUC	SEN (%)	SPE (%)	Cut-off
Training set	Intratumoural T1WI	91.7 (85.6–96.9)	0.964 (0.931–0.996)	**95.9** (91.8–98.1)	91.2 (86.3–97.6)	0.643
	Intratumoural T2WI	89.5 (84.9–93.2)	0.966 (0.943–0.989)	84.6 (75.2–88.0)	**97.1** (90.1–100)	0.669
	Peritumoural T2WI	**93.7** (88.9–97.7)	**0.975** (0.956–0.993)	93.3 (89.2–97.3)	94.1 (85.2–98.6)	0.556
Training set	Intratumoural T1WI	77.3 (70.9–83.7)	0.969 (0.942–0.997)	49.1 (41.9–67.3)	100 (98.9–100)	0.643
	Intratumoural T2WI	69.1 (62.5–75.8)	0.945 (0.904–0.986)	41.8 (39.8–61.4)	100 (99.1–100)	0.669
	Peritumoural T2WI	**87.3** (80.9–93.1)	**0.979** (0.959–0.999)	**76.4** (61.8–86.2)	**100** (97.5–100)	0.556

Statistical quantifications are reported with 95% confidence intervals. T1WI, T1-weighted imaging; T2WI, T2-weighted imaging; ACC, balanced accuracy; AUC, area under receiver operating characteristic curve; SEN, sensitivity; SPE, specificity.

Table 3
Performance of combined models.

Cohort	Model	ACC (%)	AUC	SEN (%)	SPE (%)	Cut-off
Training set	Intratumoural T1WI + Intratumoural T2WI	93.4 (88.9–96.6)	0.967 (0.929–1)	93.3 (89.2–97.2)	94.1 (84.6–100)	0.658
	Intratumoural T2WI + peritumoural T2WI	93.4 (88.9–96.6)	0.991 (0.981–1)	91.9 (85.7–95.5)	100 (94.3–100)	0.670
	Multi-sequence	**97.8** (94.5–99.4)	**0.998** (0.994–1)	**97.3** (94.2–99.4)	**100** (90.6–100)	0.594
Testing set	Intratumoural T1WI + Intratumoural T2WI	67.4 (56.8–76.8)	0.980 (0.959–1)	45.5 (32.2–58.5)	100 (93.6–100)	0.658
	Intratumoural T2WI + peritumoural T2WI	80.4 (70.9–87.9)	0.994 (0.986–1)	67.3 (56.6–81.3)	100 (98.1–100)	0.670
	Multi-sequence	**90.2** (82.2–95.4)	**0.999** (0.997–1)	**83.6** (78.2–95.3)	**100** (97.5–100)	0.594

Statistical quantifications are reported with 95% confidence intervals. T1WI, T1-weighted imaging; T2WI, T2-weighted imaging; ACC, balanced accuracy; AUC, area under receiver operating characteristic curve; SEN, sensitivity; SPE, specificity.

0.666 and 0.608 in training and testing sets. The predictive result of clinical model was significantly lower 30% than radiomic models.

4. Discussion

In this multicentre study, we investigated radiomic analysis based on pretreatment MRI scans to predict the clinical response to NACT in patients with LACC. A multi-sequence model combining the intratumoural and peritumoural regions of two radiomic sequences demonstrated the best predictive power in both training (AUC: 0.998) and testing (AUC: 0.999) sets.

In the present study, ten features were selected from the intratumoural region on T1WI, two features were selected from the intratumoural region on T2WI, and four features were selected from the peritumoural region on T2WI. Among these features, most were textural features of images, which allow multi-view description of the tumour phenotype and cannot be easily identified by humans. From the perspective of view of features, the result was similar to those of previous studies of other cancers [43,44], the features of responders presented higher textual pattern complexity or heterogeneity than those of non-responders. After the single sequence models were constructed, all models demonstrated relatively satisfactory predictive performance. Strikingly, although the peritumoural T2WI model did not carry the highest number of features, it still exhibited higher predictive power than other single sequence models. In previous studies, Braman et al. [43] comfirmed the valuable of peritumoural textural radiomic features in enhancing pCR prediction by quantitatively characterizing the presence of tumour infiltrating lymphocytes (TILs) and surrounding stromal abnormalities or responses. The study demonstrated that the peritumoural radiomics profile correspondingly captured the histological heterogeneity of TILs and micro-vascular invasion between non-pCR and pCR. Similarly, many studies [45] have proposed that the pretreatment host immune states of advanced cervical cancer could affect the treatment response to NACT. Moreover, Yun et al. [46] recently discovered a significant correlation between low peritumoural Foxp3+ infiltrating T cells and the clinical efficacy of NACT in patients with LACC. Therefore, peritumoural immunological heterogeneity between chemotherapeutic non-responders and responders was characterized by the best-performing radiomic features.

In addition, we also constructed combined models to study the impact of the combination of different regions or sequences on predictive power. The performance of the combined model of intratumoural regions was highly similar to that of the T1WI model, with no significant improvement. Surprisingly, the T2WI with intratumoural and peritumoural regions model exhibited significantly enhanced predictive performance compared to the single sequence model, with high AUCs in the training and testing sets. However, the performance of these models in terms of sensitivity was not satisfactory. They had excellent sensitivity in training set but not in testing set. Therefore, the multi-sequence model was generated, which combined all sequences and their tumour regions. The multi-sequence model exhibited the best predictive ability, which was significant higher ($p < .05$) than all other models. The accuracy, AUC, sensitivity and specificity of the multi-sequence model offered outstanding predictive power and generalization in both the training and testing sets. This indicates that the multi-sequence model can not only accurately predict the response to NACT, but also perfectly identify non-responders. This will help to protect these non-responders from NACT before treatment and avoid a delayed treatment process. By incorporating radiomic features reflecting peritumoural and tumoural heterogeneity, the multi-sequence model offered the most comprehensive and thorough radiomic assessment for predicting the clinical response to NACT and yielded excellent performance. Our results

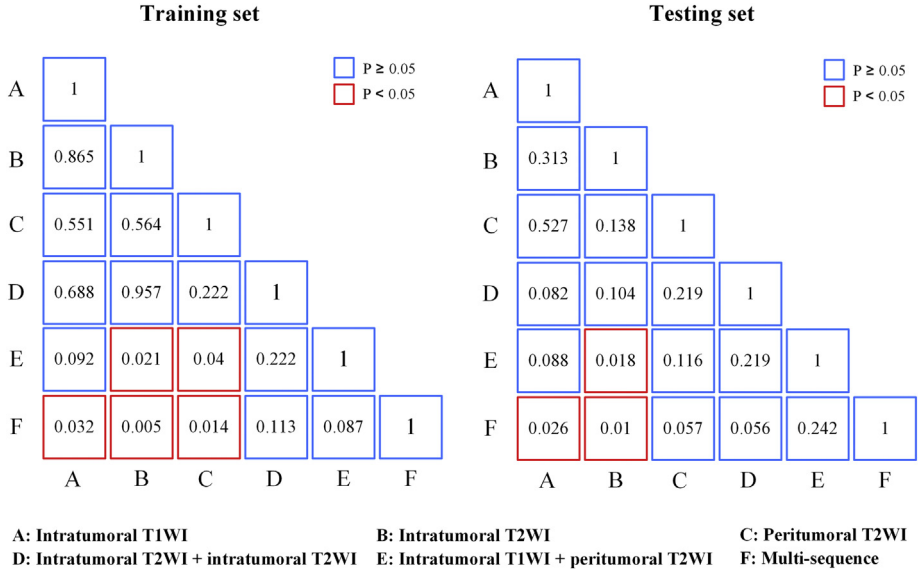

Fig. 4. Delong test between different models. P-value of Delong test between any two models. T1WI, T1-weighted imaging; T2WI, T2-weighted imaging.

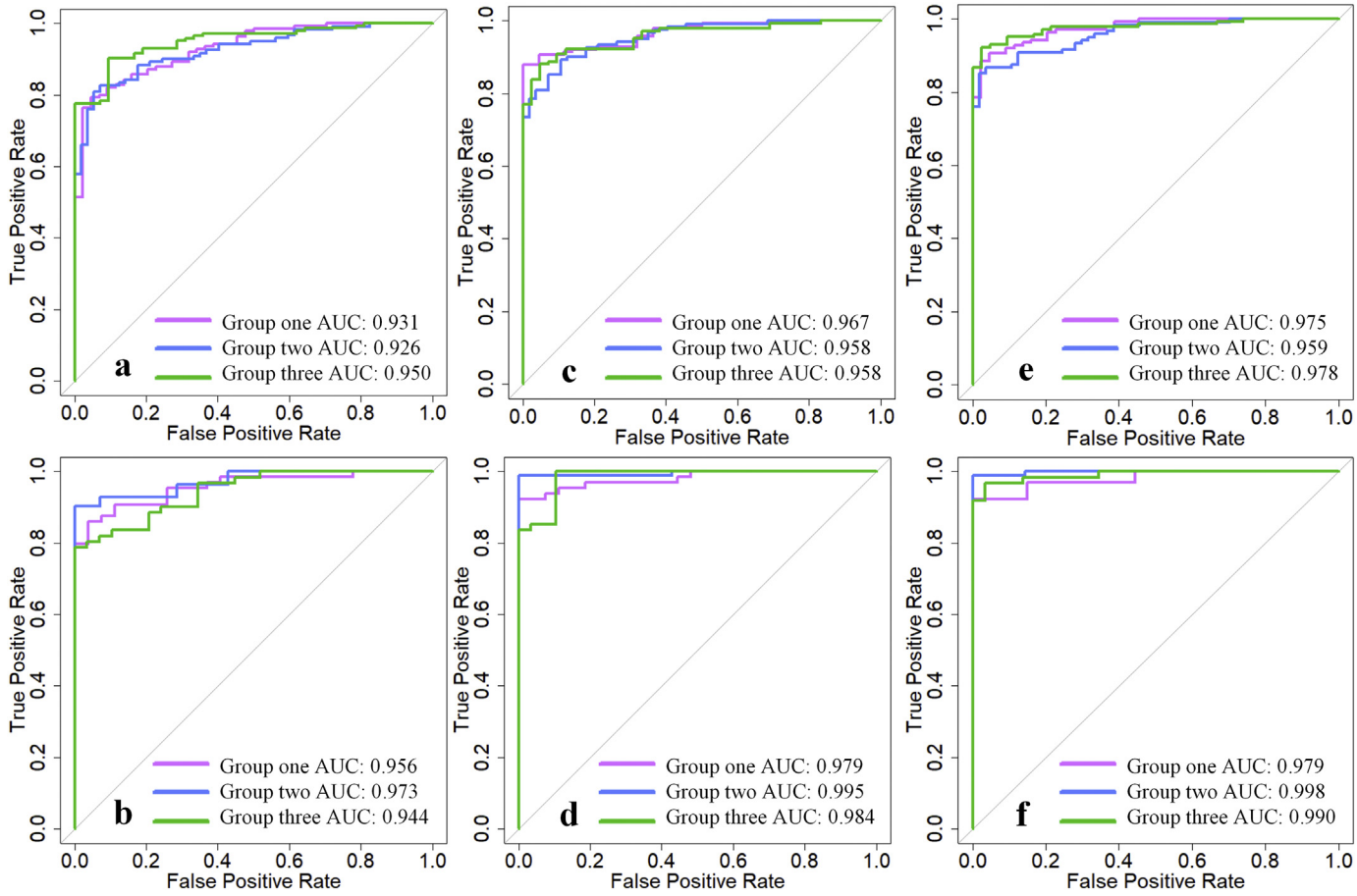

Fig. 5. Comparison of ROC curves between different group of training and testing sets for combined models. (a) and (b) are ROC curves of combined model of intratumoural region on T1WI and intratumoural region on T2WI in training and testing sets. (c) and (d) are ROC curves of combined model of peritumoural and intratumoural zones on T2WI in training and testing sets. (e) and (f) are ROC curves of multi-sequence model in training and testing sets. ROC receiver operating characteristic; AUC area under receiver operating characteristic curve; T1WI, T1-weighted imaging; T2WI, T2-weighted imaging.

provided additional evidence supporting the use of MRI in predicting the clinical response to NACT. We investigated the diagnostic robustness for response prediction of the combined models, and three various training sets constructed by different combinations of centres were applied. As indicated in Table S8, the multi-sequence model performed strong robustness in different experimental groups. The predictive accuracy of the multi-sequence model for non-responders was higher and more stable than that of other models. By comparing the information of features, some features (Table S9) were repeatedly selected in different experimental groups, such as glszm_GLV extracted from

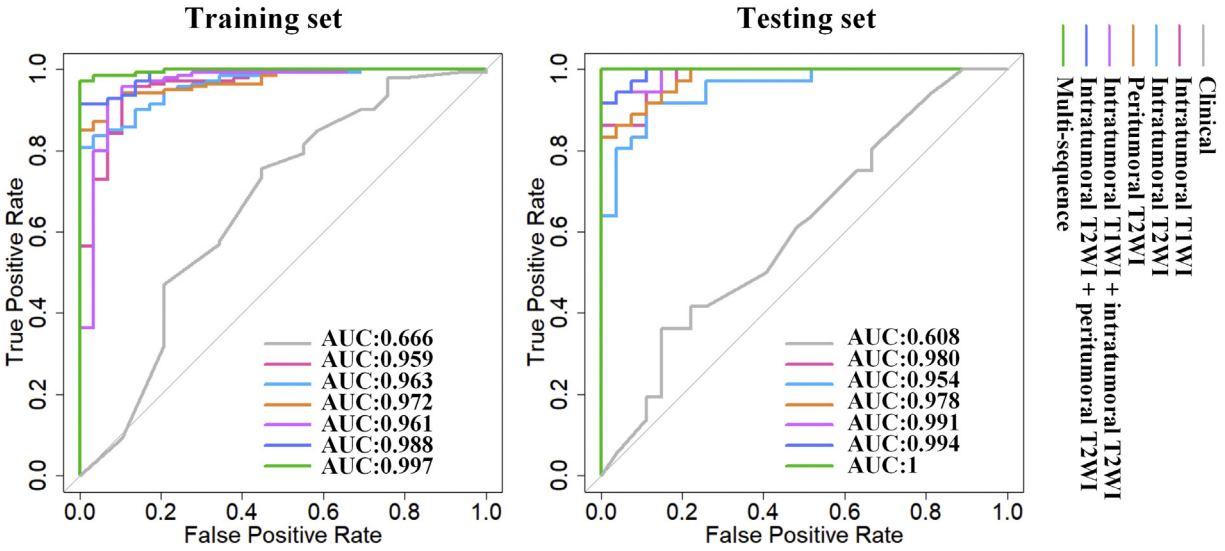

Fig. 6. Comparison of ROC curves between clinical and radiomic models. ROC receiver operating characteristic; AUC area under receiver operating characteristic curve; T1WI, T1-weighted imaging; T2WI, T2-weighted imaging.

T1WI, ngtdm_busyness extracted from intratumoural zone of T2WI, glcm_correlation extracted from intratumoural zone of T2WI, and ngtdm_complexity extracted from peritumoural of T2WI. This shows that the strong predictive power and robustness of these radiomic features in prediction of response to neoadjuvant chemotherapy in locally advanced cervical cancer. Furthermore, a clinical model was constructed based on the subset of patients whose clinical information is available. From the experimental result, the clinical factor cannot accurately predict the response to NACT.

Currently, the treatment response in cervical cancer is determined by the shrinkage of tumour size while MRI is the most effective imaging modality to assess tumour response to chemotherapy. As morphological change is not evident until completion of certain cycles of chemotherapy, chemotherapeutic non-responders cannot be earlier ruled out, resulting in increased toxicity, morbidity and worse prognosis. Some proposed imaging biomarkers from functional MRI and cellular markers such as P-Glycoprotein and proliferating cell nuclear antigen [47], squamous cell carcinoma antigen [14], and cyclooxygenase (COX)-2 ratio [48] are either limited by post- therapeutically basis or lack of validation. So far, clinical use of NACT is hampered by the lack of effective and validated pre-therapy predictors to identify suitable chemotherapeutic responders. Recently, results of phase III randomized trial [49] revealed comparable efficacy between NACT-RH and chemoradiation emphasizing the importance of remaining quality of life in treatment planning. In selected chemo-sensitive LACC patients, NACT-RH are likely to be an optimal treatment plan avoiding function loss of vaginal, ovary caused by radical radiotherapy. Therefore, a non-invasive MRI-based pre-treatment radiomics model that allows for accurate and rapid prediction of individual therapy response presented in the study would have immense value in clinical practice. Besides, several prior researchs [50,51] have investigated the predictive potential of radiomic features by combining FDG PET and MRI in lung cancer and head-and-neck cancer. Meanwhile, some metabolic radiomics features that characterizing intratumoural metabolic heterogeneity has shown to be valuable for assessing locoregional recurrences and distant metastasis after definitive chemoradiotherapy in LACC [31,52]. The further utility of radiomics based on FDG PET and MRI in the pre-therapeutically prediction of response to NACT in LACC may help to discover radiomic predictors of chemotherapeutic response that potential possesses unique prognostic information.

Our study still has some limitations despite the encouraging results. Firstly, due to the MR images being retrospectively collected from various centres with different scanners and acquisition parameters, we finally adopted a limited population size with all required sequences for model construction. Sencondly, we simplified patients' histocytes into squamous cell carcinomas only for the purposes the investigation. Therefore, the radiomic model might not be generalizable to adenocarcinoma or neuroendocrine carcinoma. Further studies with larger independent external datasets from other centres are warranted to confirm our proposed radiomic models. If possible, prospective studies are needed for further validation.

5. Conclusion

The clinical utility of neoadjuvant therapy in the treatment of advanced cervical cancer is hampered due to lack of effective predictors of response prior to the initiation of therapy. Such a predictive tool could allow for prudent selection of suitable patients for NACT while identifying non-responders for more personalized care avoiding ineffective therapies. For this purpose, we successfully combined peritumoural and intratumoural radiomics from highly heterogeneous pretreatment MRI scans to predict the clinical response to NACT with superior accuracy. The good predictive robustness of the proposed model among various centres with consistent accuracy indicated its potential for widespread adoption in clinical decision-making for NACT in patients with LACC. Our findings suggested that the radiomic model is sufficient to serve as an effective tool to stratify LACC patients to allow for more appropriate initial treatment, showing promise in improving the management of LACC.

Funding sources

This work was supported by the National Key Research and Development Plan of China [Grant No. 2017YFA0205200]; the National Natural Science Foundation of China [Grant No. 81772012, 81227901, 81527805, and 66161010]; the Nature Science Foundation of Guizhou province [Grant No. 20152044]; the Chinese Academy of Sciences [Grant No. GJJSTD20170004, XDB32030200, and QYZDJ-SSW-JSC005]; the Beijing Natural Science Foundation [Grant No. 7182109]; the Youth Innovation Promotion Association CAS [Grant No. 2019136]. The National Natural Science Foundation of Guangdong [Grant No. 2015A030311024]; the Health and Medical Cooperation Innovation Special Program of Guangzhou Municipal Science and Technology [No. 201508020264]; the National Key Technology Program of the Ministry of Science and Technology [863 program, Grant No. 2014BAI05B03]; the Medical Scientific Research Foundation of Guangdong Province of China [Grant No. A2015063]. The funders had no role in study design, data collection, data analysis, interpretation, writing of the report.

Declaration of Competing Interests

The authors declare no potential conflicts of interest.

Author contributions

Conception and design: Chunlin Chen, Jie Tian.

Collection and assembly of data: Xin Tian, Weili Li, Pengfei Li, Jiaming Chen, Weifeng Zhang, Ziyu Fang, Peiyan Du, Hui Duan.

Development of methodology: Chunlin Chen, Lihui Wang, Ping Liu, Weili Li, Zhenyu Liu, Caixia Sun, Xin Tian.

Data analysis and interpretation: Caixia Sun, Xin Tian, Zhenyu Liu, Weili Li, Ping Liu, Lihui Wang, Chunlin Chen, Jie Tian.

Manuscript writing: All authors.

Final approval of manuscript: All authors.

Appendix A. Supplementary data

Supplementary data to this article can be found online at https://doi.org/10.1016/j.ebiom.2019.07.049.

References

[1] Siegel RL, Miller KD, Jemal A. Cancer statistics, 2019. CA Cancer J Clin 2019;69:7–34. https://doi.org/10.3322/caac.21551.
[2] Bhatla N, Aoki D, Sharma DN, Sankaranarayanan R. Cancer of the cervix uteri. Int J Gynecol Obstet 2018;143:22–36. https://doi.org/10.1002/ijgo.12611.
[3] DeSouza NM, Soutter WP, Rustin G, Mahon MM, Jones B, Dina R, et al. Use of neoadjuvant chemotherapy prior to radical hysterectomy in cervical cancer: monitoring tumour shrinkage and molecular profile on magnetic resonance and assessment of 3-year outcome. Br J Cancer 2004;90:2326–31. https://doi.org/10.1038/sj.bjc.6601870.
[4] Yang Z, Chen D, Zhang J, Yao D, Gao K, Wang H, et al. The efficacy and safety of neoadjuvant chemotherapy in the treatment of locally advanced cervical cancer: a randomized multicenter study. Gynecol Oncol 2016;141:231–9. https://doi.org/10.1016/j.ygyno.2015.06.027.
[5] Angioli R, Plotti F, Montera R, Aloisi A, Luvero D, Capriglione S, et al. Neoadjuvant chemotherapy plus radical surgery followed by chemotherapy in locally advanced cervical cancer. Gynecol Oncol 2012;127:290–6. https://doi.org/10.1016/j.ygyno.2012.07.104.
[6] Hu T, Li S, Chen Y, Shen J, Li X, Huang K, et al. Matched-case comparison of neoadjuvant chemotherapy in patients with FIGO stage IB1-IIB cervical cancer to establish selection criteria. Eur J Cancer 2012;48:2353–60. https://doi.org/10.1016/j.ejca.2012.03.015.
[7] Scambia G, Benedetti Panici P, Foti E, Amoroso M, Salerno G, Ferrandina G, et al. Squamous cell carcinoma antigen: prognostic significance and role in the monitoring of neoadjuvant chemotherapy response in cervical cancer. J Clin Oncol 1994;12:2309–16. https://doi.org/10.1200/JCO.1994.12.11.2309.

[8] Chen H, Liang C, Zhang L, Huang S, Wu X. Clinical efficacy of modified preoperative neoadjuvant chemotherapy in the treatment of locally advanced (stage IB2 to IIB) ervical ancer: randomized study. Gynecol Oncol 2008;110:308–15. https://doi.org/10.1016/j.ygyno.2008.05.026.

[9] Katsumata N, Yoshikawa H, Kobayashi H, Saito T, Kuzuya K, Nakanishi T, et al. Phase III randomised controlled trial of neoadjuvant chemotherapy plus radical surgery vs radical surgery alone for stages IB2, IIA2 and IIB cervical cancer: a Japan clinical oncology group trial (JCOG 0102). Br J Cancer 2013;108:1957–63. https://doi.org/10.1038/bjc.2013.179.

[10] Harry VN, Semple SI, Gilbert FJ, Parkin DE. Diffusion-weighted magnetic resonance imaging in the early detection of response to chemoradiation in cervical cancer. Gynecol Oncol 2008;111:213–20. https://doi.org/10.1016/j.ygyno.2008.07.048.

[11] Tanderup K, Fokdal LU, Sturdza A, Haie-Meder C, Mazeron R, van Limbergen E, et al. Effect of tumor dose, volume and overall treatment time on local control after radiochemotherapy including MRI guided brachytherapy of locally advanced cervical cancer. Radiother Oncol 2016;120:441–6. https://doi.org/10.1016/j.radonc.2016.05.014.

[12] Zhang W, Chen C, Liu P, Li W, Hao M, Zhao W, et al. Impact of pelvic MRI in routine clinical practice on staging of IB1-IIA2 cervical cancer. Cancer Manage Res 2019;11:3603–9. https://doi.org/10.2147/CMAR.S197496.

[13] Zhang W, Chen C, Liu P, Li W, Hao M, Zhao W, et al. Staging early cervical cancer in China: data from a multicenter collaborative. Int J Gynecol Cancer 2019;29:869–73. https://doi.org/10.1136/ijgc-2019-000263.

[14] Yin M, Hou Y, Zhang T, Cui C, Zhou X, Sun F, et al. Evaluation of chemotherapy response with serum squamous cell carcinoma antigen level in cervical Cancer patients: a prospective cohort study. PLoS One 2013;8. https://doi.org/10.1371/journal.pone.0054969.

[15] Fu C, Bian D, Liu F, Feng X, Du W, Wang X. The value of diffusion-weighted magnetic resonance imaging in assessing the response of locally advanced cervical cancer to neoadjuvant chemotherapy. Int J Gynecol Cancer 2012;22:1037–43. https://doi.org/10.1097/IGC.0b013e31825736d7.

[16] Himoto Y, Fujimoto K, Kido A, Matsumura N, Baba T, Daido S, et al. Assessment of the early predictive power of quantitative magnetic resonance imaging parameters during neoadjuvant chemotherapy for uterine cervical cancer. Int J Gynecol Cancer 2014;24:751–7. https://doi.org/10.1097/IGC.0000000000000124.

[17] Zhu L, Zhu L, Shi H, Wang H, Yan J, Liu B, et al. Evaluating early response of cervical cancer under concurrent chemo-radiotherapy by intravoxel incoherent motion MR imaging. BMC Cancer 2016;16:1–8. https://doi.org/10.1186/s12885-016-2116-5.

[18] Lambin P, Rios-Velazquez E, Leijenaar R, Carvalho S, Van Stiphout RGPM, Granton P, et al. Radiomics: extracting more information from medical images using advanced feature analysis. Eur J Cancer 2012;48:441–6. https://doi.org/10.1016/j.ejca.2011.11.036.

[19] Aerts HJWL, Velazquez ER, Leijenaar RTH, Parmar C, Grossmann P, Cavalho S, et al. Decoding tumour phenotype by noninvasive imaging using a quantitative radiomics approach. Nat Commun 2014;5. https://doi.org/10.1038/ncomms5006.

[20] Liu Z, Wang S, Dong D, Wei J, Fang C, Zhou X, et al. The applications of Radiomics in precision diagnosis and treatment of oncology: opportunities and challenges. Theranostics 2019;9:1303–22. https://doi.org/10.7150/thno.30309.

[21] Tang Z, Liu Z, Li R, Yang X, Cui X, Wang S, et al. Identifying the white matter impairments among ART-naïve HIV patients: a multivariate pattern analysis of DTI data. Eur Radiol 2017;27:4153–62. https://doi.org/10.1007/s00330-017-4820-1.

[22] Tian Y, Liu Z, Tang Z, Li M, Lou X, Dong E, et al. Radiomics analysis of DTI data to assess vision outcome after intravenous methylprednisolone therapy in Neuromyelitis optic neuritis. J Magn Reson Imaging 2018;49:1365–73. https://doi.org/10.1002/jmri.26326.

[23] Wei W, Liu Z, Rong Y, Zhou B, Bai Y, Wei W, et al. A computed tomography-based radiomic prognostic marker of advanced high-grade serous ovarian cancer recurrence: a multicenter study. Front Oncol 2019;9:1–12. https://doi.org/10.3389/fonc.2019.00255.

[24] Wang S, Shi J, Ye Z, Dong D, Yu D, Zhou M, et al. Predicting EGFR mutation status in lung adenocarcinoma on CT image using deep learning. Eur Respir J 2019:1800986. https://doi.org/10.1183/13993003.00986-2018.

[25] Tang Z, Zhang XY, Liu Z, Li XT, Shi YJ, Wang S, et al. Quantitative analysis of diffusion weighted imaging to predict pathological good response to neoadjuvant chemoradiation for locally advanced rectal cancer. Radiother Oncol 2019;132:100–8. https://doi.org/10.1016/j.radonc.2018.11.007.

[26] Zhou X, Yi Y, Liu Z, Cao W, Lai B, Sun K, et al. Radiomics-based Pretherapeutic prediction of non-response to Neoadjuvant therapy in locally advanced rectal cancer. Ann Surg Oncol 2019. https://doi.org/10.1245/s10434-019-07300-3.

[27] Antunovic L, De Sanctis R, Cozzi L, Kirienko M, Sagona A, Torrisi R, et al. PET/CT radiomics in breast cancer: promising tool for prediction of pathological response to neoadjuvant chemotherapy. Eur J Nucl Med Mol Imaging 2019. https://doi.org/10.1007/s00259-019-04313-8.

[28] Liu Z, Li Z, Qu J, Zhang R, Zhou X, Li L, et al. Radiomics of multi-parametric MRI for pretreatment prediction of pathological complete response to neoadjuvant chemotherapy in breast cancer: A multicenter study. Clin Cancer Res 2019:Clincanres 2018;vol. 3190. https://doi.org/10.1158/1078-0432.CCR-18-3190.

[29] El Naqa I, Grigsby PW, Apte A, Kidd E, Donnelly E, Khullar D, et al. Exploring feature-based approaches in PET images for predicting cancer treatment outcomes. Pattern Recognit 2009;42:1162–71. https://doi.org/10.1016/j.patcog.2008.08.011.

[30] Lucia F, Visvikis D, Miranda O, Desseroit MC, Robin P, Pradier O, et al. PO-0805: prediction of outcome using pretreatment PET and MRI radiomics in locally advanced cervical cancer. Eur J Nucl Med Mol Imaging 2018;127:S419. https://doi.org/10.1016/S0167-8140(18)31115-0.

[31] Lucia F, Visvikis D, Vallières M, Desseroit M, Miranda O, Robin P, et al. External validation of a combined PET and MRI radiomics model for prediction of recurrence in cervical cancer patients treated with chemoradiotherapy. Eur J Nucl Med Mol Imaging 2018. https://doi.org/10.1007/s00259-018-4231-9.

[32] Eisenhauer EA, Therasse P, Bogaerts J, Schwartz LH, Sargent D, Ford R, et al. New response evaluation criteria in solid tumours: revised RECIST guideline (version 1.1). Eur J Cancer 2009;45:228–47. https://doi.org/10.1016/j.ejca.2008.10.026.

[33] Martin V, Alex Z, Bodgan B, Le Catherine Cheze, Rest Dimitris V, Mathieu H. Responsible radiomics research for faster clinical translation. J Nucl Med 2018;59:189–93. https://doi.org/10.2967/jnumed.117.200501.

[34] Zwanenburg A, Leger S, MLS Vallieres. Image biomarker standardisation initiative. ArXiv Preprint arXiv:161207003 2016https://arxiv.org/abs/1612.07003.

[35] Chatterjee A, Vallieres M, Dohan A, Levesque IR, Ueno Y, Saif S, et al. Creating robust predictive Radiomic models for data from independent institutions using normalization. IEEE Trans Radiat Plasma Med Sci 2019;3:210–5. https://doi.org/10.1109/trpms.2019.2893860.

[36] Huang ML, Hung YH, Lee WM, Li RK, Jiang BR. SVM-RFE based feature selection and taguchi parameters optimization for multiclass SVM classifier. Sci World J 2014;2014. https://doi.org/10.1155/2014/795624.

[37] Zhang X, Xu X, Tian Q, Li B, Wu Y, Yang Z, et al. Radiomics assessment of bladder cancer grade using texture features from diffusion-weighted imaging. J Magn Reson Imaging 2017;46:1281–8. https://doi.org/10.1002/jmri.25669.

[38] Xu X, Zhang X, Tian Q, Wang H, Cui LB, Li S, et al. Quantitative identification of nonmuscle-invasive and muscle-invasive bladder carcinomas: a multiparametric MRI Radiomics analysis. J Magn Reson Imaging 2018:1–10. https://doi.org/10.1002/jmri.26327.

[39] Fawcett T. An introduction to ROC analysis. Pattern Recognit Lett 2006;27:861–74. https://doi.org/10.1016/j.patrec.2005.10.010.

[40] Youden WJ. Index for rating diagnostic tests. Cancer 1950:32–5.

[41] DeLong Elizabeth R. David M. DeLong DLC-P. comparing the areas under two or more correlated receiver operating characteristic curves: a nonparametric approach. Biometrics 1988;44:837–45.

[42] Brodersen KH, Ong CS, Stephan KE, Buhmann JM. The balanced accuracy and its posterior distribution. Proc - Int Conf Pattern Recognit 2010:3121–4. https://doi.org/10.1109/ICPR.2010.764.

[43] Braman NM, Etesami M, Prasanna P, Dubchuk C, Gilmore H, Tiwari P, et al. Intratumoral and peritumoral radiomics for the pretreatment prediction of pathological complete response to neoadjuvant chemotherapy based on breast DCE-MRI. Breast Cancer Res 2017;19:1–14. https://doi.org/10.1186/s13058-017-0846-1.

[44] Khorrami M, Thawani R, Madabhushi A. Combination of peri- and intratumoral radiomic features on baseline CT scans predicts response to chemotherapy in lung adenocarcinoma. Radiol Artif Intell 2019;1.

[45] Castellano T, Moore KN, Holman LL. An overview of immune checkpoint inhibitors in gynecologic cancers. Clin Ther 2018;40:372–88. https://doi.org/10.1016/j.clinthera.2018.01.005.

[46] Liang Y, Lü W, Zhang X, Lü B. Tumor-infiltrating CD8+ and FOXP3+ lymphocytes before and after neoadjuvant chemotherapy in cervical cancer. Diagn Pathol 2018;13:1–8. https://doi.org/10.1186/s13000-018-0770-4.

[47] Konishi I, Nanbu K, Mandai M, Tsuruta Y, Kataoka N, Nagata Y, et al. Tumor response to neoadjuvant chemotherapy correlates with the expression of P-glycoprotein and PCNA but not GST-π in the tumor cells of cervical carcinoma. Gynecol Oncol 1998;70:365–71. https://doi.org/10.1006/gyno.1998.5077.

[48] Ferrandina G, Ranelletti FO, Legge F, Gessi M, Salutari V, Distefano MG, et al. Prognostic role of the ratio between cyclooxygenase-2 in tumor and stroma compartments in cervical cancer. Clin Cancer Res 2004;10:3117–23. https://doi.org/10.1158/1078-0432.CCR-1090-3.

[49] Gupta S, Maheshwari A, Parab P, Mahantshetty U, Hawaldar R, Sastri S, et al. Neoadjuvant Chemotherapy Followed by Radical Surgery Versus Concomitant Chemotherapy and Radiotherapy in Patients With Stage IB2, IIA, or IIB Squamous Cervical Cancer: A Randomized Controlled Trial. J Clin Oncol 2018;36:1548–55. https://doi.org/10.1200/JCO.2017.75.9985.

[50] Vallières M, Freeman CR, Skamene SR, El Naqa I. A radiomics model from joint FDG-PET and MRI texture features for the prediction of lung metastases in soft-tissue sarcomas of the extremities. Phys Med Biol 2015;60:5471–96. https://doi.org/10.1088/0031-9155/60/14/5471.

[51] Vallières M, Kay-Rivest E, Perrin LJ, Liem X, Furstoss C, Aerts HJWL, et al. Radiomics strategies for risk assessment of tumour failure in head-and-neck cancer. Sci Rep 2017;7:10117. https://doi.org/10.1038/s41598-017-10371-5.

[52] Shen W, Chen S, Wu K, Hsieh T, Liang J, Hung Y. Prediction of local relapse and distant metastasis in patients with definitive chemoradiotherapy-treated cervical cancer by deep learning from [18 F] -fluorodeoxyglucose positron emission tomography / computed tomography. Eur Radiol 2019. https://doi.org/10.1007/s00330-019-06265-x.